

SCIENTIFIC REPORTS



OPEN

The interplay between p16 serine phosphorylation and arginine methylation determines its function in modulating cellular apoptosis and senescence

Received: 17 August 2016
Accepted: 20 December 2016
Published: 25 January 2017

Yang Lu¹, Wenlong Ma¹, Zhongwei Li¹, Jun Lu¹ & Xiuli Wang^{1,2}

Cyclin-dependent kinase inhibitor p16^{INK4a} (p16) primarily functions as a negative regulator of the retinoblastoma protein (Rb) -E2F pathway, thus plays critical role in cell cycle progression, cellular senescence and apoptosis. In this study, we showed that the methylation of Arg 138 and the phosphorylation of Ser 140 on p16 were critical for the control of cell proliferation and apoptosis. Compared to wild type p16, mutant p16R138K possessed improved function in preventing cell proliferation and inducing apoptosis, while the Ser 140 mutation (p16S140A) exhibited the opposite alteration. We also demonstrated that H₂O₂ was able to induce the phosphorylation of p16, which facilitated the interaction between CDK4 (Cyclin-dependent protein kinase) and p16, in 293T (human embryonic kidney) cells. Furthermore, the elevated arginine methylation in p16S140A mutant and increased serine phosphorylation in p16R138K mutant suggest that a antagonizing mechanism coordinating Arg 138 methylation and Ser 140 phosphorylation to regulates p16 function as well as cellular apoptosis and senescence. These findings will therefore contribute to therapeutic treatment for p16-related gene therapy by providing theoretical and experimental evidence.

The p16 protein inhibits the activity of cyclin-dependent protein kinases (CDK4 and CDK6) to prevent the phosphorylation of the retinoblastoma protein (Rb) and subsequently lead to the accumulation of the hypophosphorylated form of Rb that mediates cell-cycle arrest¹. Studies have shown that abnormal expression of p16 is frequently associated with different types of human tumors, such as melanoma, non-small cell lung carcinoma, breast cancer, colorectal cancer, bladder cancer and squamous cell carcinoma of the head and neck²⁻⁴.

Multiple mechanisms, including transcriptional regulation, DNA mutation and promoter methylation, are involved in the control of p16 expression. It has been demonstrated that various transcription factors, such as Ets and Bmi1, play critical roles in the transcriptional regulation p16 gene⁵. Our earlier studies showed that the histone acetyltransferase p300 recruited by Sp1 stimulated p16 transcription through inducing the H4 hyperacetylation on p16 gene, whereas HDAC3/4 inhibited the p16 promoter activity via the transcription factors YY1 and ZBP-89⁶⁻⁸.

Interestingly, recent work found that p16 phosphorylation increased in senescent human prostatic epithelial cells⁹. Subsequently, four phosphorylation sites, including Ser 7, Ser 8, Ser 140 and Ser 152, on p16 protein have been identified in human fibroblast cells, among these sites, only phosphorylated Ser 152 was detected in CDK4/6-bound p16¹⁰. In addition, another report showed that p16 phosphorylation at Ser 8 catalyzed by IKK β relieved p16-mediated CDK4 inhibition¹¹. Recently, we have demonstrated that p16 are methylated at Arg 22, Arg 131 and Arg 138 by PRMT6 and these modifications alleviated the cell cycle arrest at G1 via reducing p16-CDK4 interaction¹². These evidence suggests important roles of post-translational modifications (PTMs) in the regulation of p16 function and cell fate.

¹The Institute of Genetics and Cytology, Northeast Normal University, Changchun 130024, P. R. China. ²School of Life Sciences, Northeast Normal University, Changchun 130024, P. R. China. Correspondence and requests for materials should be addressed to X.W. (email: wangxl034@nenu.edu.cn)

A previous report showed that the arginine residues of FOXO1 was methylated by PRMT1, and this modification blocked the Akt-mediated phosphorylation of serine sites of the protein¹³. Moreover, PRMT1-mediated methylation of two arginine residues (Arg 94 and Arg 96) inhibited Akt-mediated phosphorylation of BAD at Ser 99 *in vitro* and *in vivo*¹⁴. It has also been shown that methylated Arg 1175 of EGFR mediated by PRMT5 positively modulates the EGF-induced EGFR trans-autophosphorylation at Tyr 1173¹⁵. These studies suggest that the interplays between arginine methylation and serine phosphorylation, especially at the neighboring positions, may be crucial to the functions of the proteins. Although p16 bears phosphorylated serines and/or methylated arginines, the crosstalk between these PTMs and its cellular functions still remain elusive.

In this study, we showed that the phosphorylation of p16 accumulated upon H₂O₂ in 293T cells. The phosphorylated forms of p16 gained increased binding affinity to CDK4 and appeared to be prone to protein degradation. Moreover, our data demonstrated that the level of arginine methylation on p16 increased as Ser 140 was replaced by alanine. Compare to wild type p16, this mutant led to alleviated cell cycle arrest and apoptosis. In contrast, the upregulated serine phosphorylation in p16R138K mutant was associated with enhanced cell cycle arrest and apoptosis. Taken together, our data outline a model where antagonistic crosstalk between Ser 140 phosphorylation and Arg 138 methylation orchestrates p16 to affect cell proliferation and apoptosis.

Results

Mutations of serines and arginines on p16 have different impacts on cell proliferation and apoptosis.

A previous study demonstrated that p16 was phosphorylated at Ser 7, Ser 8, Ser 140 and Ser 152 in human fibroblast cells¹⁰. It seemed that these phosphorylation sites influenced p16 function differently^{10,11}. Moreover, our previous study showed that methylation at Arg 22, Arg 131 and Arg 138 inhibited the activity of p16 to relieve the cell cycle arrest at G1 phase¹². However, whether serine phosphorylation is coordinated with arginine methylation to control p16 function has not been characterized. To gain more insights into this issue, we mutated serine to alanine at different sites, including p16S8, p16S140 and p16S152 using pWPXLD-p16 expression plasmid. Subsequently, these mutants along with previously generated p16R138K, p16R22K/R131K/R138K (p16KKK) and p16R138K/S140A were expressed with comparable levels in 293T cells (Fig. 1A). As expected, the overexpression of wild type p16 caused an accumulation of cells in G1 phase (53.298%) as compared to the control (41.675%). Interestingly, the R138 mutant (p16R138K) and the triple arginine mutant (p16KKK) increased the population of G1 cells to 57.412% and 59.538%, while p16S8A and p16S140A had the opposite effect resulting in 49.344% and 45.796% G1 cells respectively (Fig. 1B). Notably, cells transfected with double mutant p16S140A/R138K displayed a similar G1 population (53.3%) to that of the wild type p16 (53.29%). It argues that the Arg 138 and Ser 140 of p16 may possess completely different functions in regulating p16 activity and the cell cycle. Moreover, the arginine mutants of p16 enhanced apoptosis as compared to wild type p16 in 293T cells. Under the same condition, p16 serine mutants reduced the apoptosis (Fig. 1C). Together, these results demonstrate that the arginine mutants (p16R138K and p16KKK) and serine mutant (p16S140A) of p16 have the opposite effect on cell cycle arrest and apoptosis.

H₂O₂ enhances the phosphorylation of p16 to promote apoptosis. H₂O₂ has been shown to induce cell apoptosis, where p16 plays a crucial role^{6,16}. Given a correlation between apoptosis and p16 phosphorylation was observed, we asked whether H₂O₂ could influence the phosphorylation of p16. To this end, we applied H₂O₂ in different doses (0.6, 0.8, 1, 1.2 and 1.4 mM) to 293T cells, in which the level of p16 phosphorylation is low (Data not shown). H₂O₂ from 0.6 to 1 mM induced cell apoptosis in a dose-dependent manner (Fig. 2A) and 1 mM H₂O₂ appeared to be the most effective dose for inducing cell apoptosis. Meanwhile, we observed that mitochondrial superoxide was increased and the mitochondria membrane potential was decreased in cells treated with H₂O₂ (Fig. 2B and C). A drastically increase of phosphorylation in endogenous p16 upon H₂O₂ treatment (Fig. 2D and Fig. S1 in the Supplementary Information) revealed H₂O₂ as an effective inducer of p16 phosphorylation. To substantiate the involvement of oxidative stress resulted from ROS generation in the H₂O₂-induced p16 phosphorylation, NAC (N-acetyl-L-cysteine, a general antioxidant) was used. The results from CoIP assays showed that NAC treatment significantly reduced H₂O₂-induced p16 phosphorylation and apoptosis (Fig. 2E and F, Fig. S2 in the Supplementary Information), suggesting that oxidative stress plays an essential role in the induction of p16 phosphorylation and apoptosis.

Phosphorylated p16 is preferentially associated with CDK4. Given that p16 function is tightly associated with CDK4, a key regulator of cell cycle progression, we next investigated whether the phosphorylation of p16 affected the interaction between p16 and CDK4. Upon H₂O₂ treatment for 24 or 48 h, more phosphorylated p16 was detected in the complex immunoprecipitated by anti-p16 antibody as expected (Fig. 3A and Fig. S3 in the Supplementary Information). Importantly, the level of CDK4 was increased significantly in cells stimulated with H₂O₂ as compared to that in untreated cells (Fig. 3A). A reciprocal immunoprecipitation by CDK4 confirmed that phosphorylated p16 was indeed increased in the p16-CDK4 complexes in response to H₂O₂ (Fig. 3B and Fig. S4 in the Supplementary Information). These data suggest that the hyper-phosphorylated p16 proteins possess upregulated CDK4-binding ability. However, the CoIP assays demonstrated that the p16S140A interacted with less CDK4 than wild type p16 without or with H₂O₂ treated (Fig. 3C and Fig. S8 in the Supplementary Information). Notably, the total p16 proteins were reduced upon the H₂O₂ treatment (Fig. 2D, E and 3A), indicating that p16 may be degraded after H₂O₂ treatment. In contrast to other critical cell cycle regulators, including p53 and p21, the level of p16 decreased by H₂O₂ treatment and restored in the presence of MG132, a widely used proteasome inhibitor (Fig. 3D and Fig. S5 in the Supplementary Information). Collectively, these data suggest that increased serine phosphorylation facilitates the association of CDK4 with p16 and the degradation of p16 can be triggered by H₂O₂.

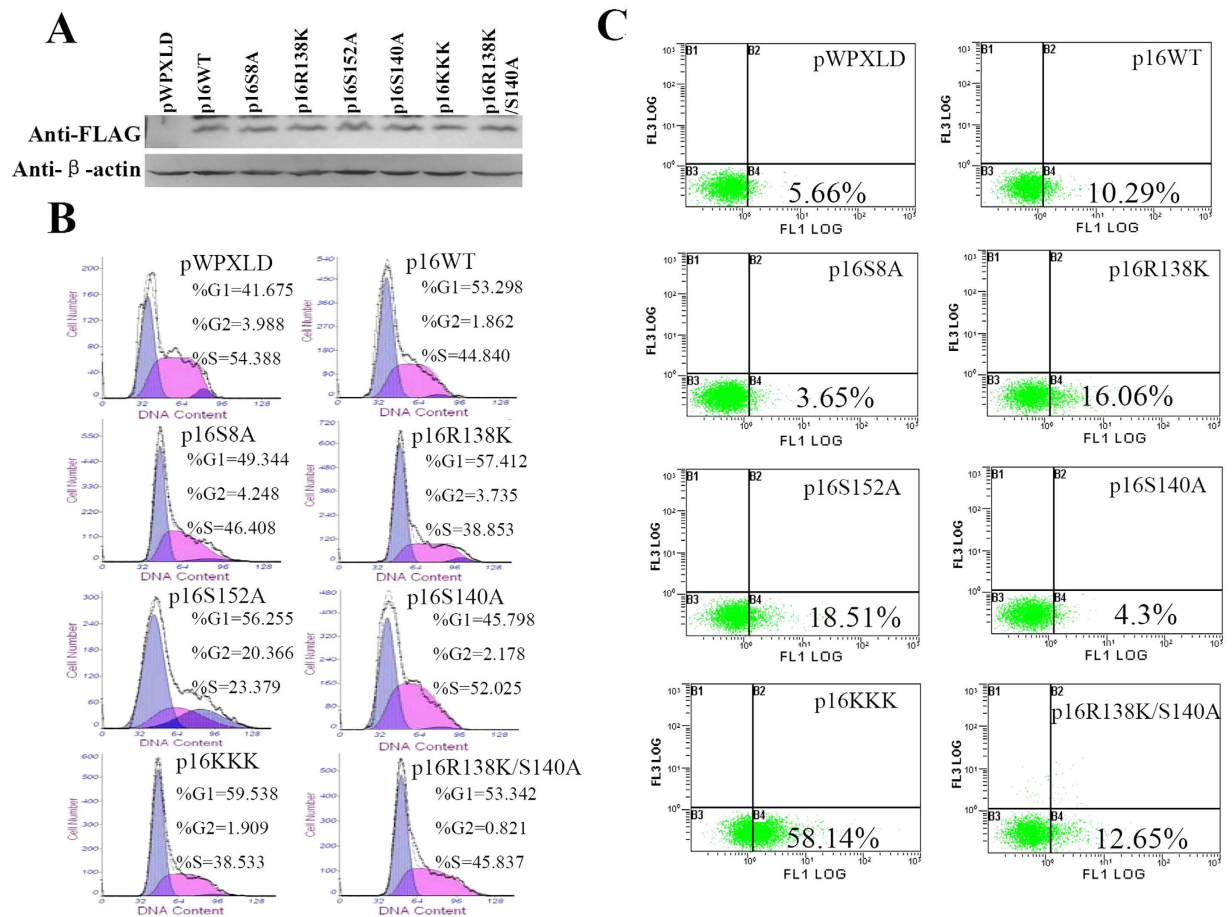


Figure 1. The serine and arginine site mutants of p16 protein exhibited different functions in cell proliferation and apoptosis. (A) Western blotting analysis of the p16 protein in 293T cells transfected with wild type p16 or mutant p16 expression plasmids, or empty control vector (pWPXLD) as a control. Flow cytometric analysis of cell cycle changes (B) and the apoptosis (C) after transfection of 293T cells with empty control vector (pWPXLD), wild type p16 or mutant p16 expression plasmids. (B) Cells were harvested at 48 h after transfection and stained with PI, analyzed by flow cytometry. (C) Cell apoptosis was measured by flow cytometry after annexin V and propidium iodide (PI) double staining after transfection 48 h.

Ser 140 phosphorylation antagonizes with the Arg 138 methylation on p16. To understand how arginine and serine modifications are coordinated to regulate p16 function in apoptosis, we ectopically overexpressed different p16 mutants in 293T cells and subsequently treated those cells with H_2O_2 . As expected, H_2O_2 efficiently caused cell apoptosis (35.67%) (Fig. 4A), while only 5.66% apoptotic cells were scored in the control (Fig. 1C). Compared to wild type p16, arginine or serine mutants, especially p16R138K and p16KKK, enhanced cell apoptosis induced by H_2O_2 (Fig. 4A). In contrast, the expression of p16S140A mutant reduced apoptotic cells to 23.98% (Fig. 4A). Additionally, the percentage of apoptotic cells induced by p16S140A/R138K mutant was close to that of cells overexpressing wild type p16 (Fig. 4A), suggesting that the Ser 140 mutant might counteract the apoptosis induced by Arg 138 mutant. Next, we asked whether an interplay between methylation and phosphorylation existed on p16. Analysis of methylated and phosphorylated p16 mutants immunoprecipitated by anti-p16 antibody demonstrated that arginine methylation in p16S140A was increased as compared to that in wild type p16 (Fig. 4B and C, lane 2 compared with lane 1 in line 2) (Fig. S9 and S6 in the Supplementary Information). In parallel, serine phosphorylation in p16R138K and p16KKK were higher than that in wild type p16 with or without H_2O_2 treated (Fig. 4B and C, lane 4 compared with lane 1 in line 1). These results implicate that an antagonistic mechanism coordinates Arg 138 methylation with Ser 140 phosphorylation on p16.

H_2O_2 induced cell senescence is accompanied by p16 phosphorylation. The critical role of p16 in cell senescence has been well established¹⁷. We thus decided to examine the H_2O_2 -dependent p16 function in cell senescence. We found that p16 overexpression or H_2O_2 treatment alone induced senescence in WI-38 cells and the combination of both resulted in an additive effect (Fig. 5A). Meanwhile, the senescence-associated heterochromatin foci (SAHF) assay confirmed the observations in senescence cell staining. Both 3MeK9H3 and HMGA1, two classic markers of SAHF, localized to the specific heterochromatic foci in cells transfected with p16 and treated with H_2O_2 (Fig. 5B). The colocalization of them in discrete foci became more obvious when p16

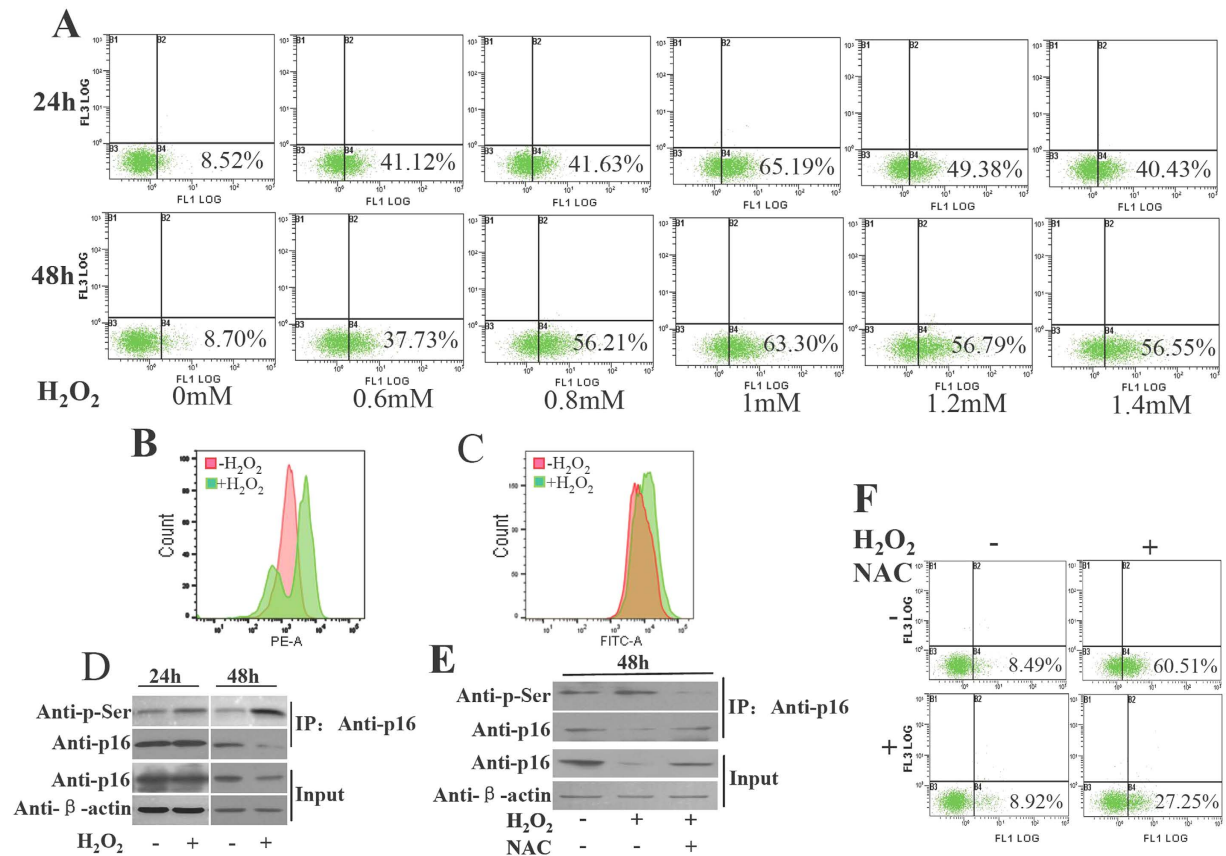


Figure 2. H₂O₂ enhanced the phosphorylation of p16 protein to promote apoptosis in 293T cells.

(A) H₂O₂ induced apoptosis in 293T cells. 293T cells were treated with different concentration of H₂O₂ (0.6 mM, 0.8 mM, 1 mM, 1.2 mM or 1.4 mM) for 24 h or 48 h, and apoptosis was evaluated by flow cytometry. Apoptosis rates were calculated on the basis of 15 000 cells. (B,C) The 293T cells were treated 1 mM H₂O₂ for 24 h and then detected by ROS in mitochondria (B) and mitochondria membrane potential (C). (D) Immunoblots showing that the H₂O₂-induced serine phosphorylation of p16. Cell extracts were prepared and precipitated with anti-p16 antibody, then detected with anti-p16 antibody or anti-phosphoserine antibody. (E) 293T cell extracts were prepared and precipitated with anti-p16 antibody, then detected in immunoblotting with anti-p16 antibody or anti-phosphoserine antibody. Cells were treated with H₂O₂ or NAC and H₂O₂. Upper panel: samples co-immunoprecipitated with antibodies; Lower panel: proteins prior to immunoprecipitation (input). (F) Cells were treated with H₂O₂ or NAC, or a combination of both (cells were treated with 30 mM NAC for 2 h and then 1 mM H₂O₂ was added). After 30 min treated with H₂O₂ the cells were cultured in normal medium for 48 h. The apoptosis was evaluated by flow cytometry.

overexpression and H₂O₂ treatment were applied together (Fig. 5B). These results indicate that overexpression of p16 and H₂O₂ treatment can induce WI-38 cell senescence. Consistent with the observations in 293T cells, our CoIP experiments showed that the level of p16 phosphorylation and the association of CDK4 with p16 increased upon the H₂O₂ treatment in WI-38 cells (Fig. 5C and Fig. S7 in the Supplementary Information). Taken together, these data suggest an important role of H₂O₂-induced p16 phosphorylation in cell senescence.

Discussion

p16 is well known as a negative regulator of the cell cycle and aberrantly expressed in various malignancies¹⁸. Previous studies have shown that the inactivation of p16 is mediated through distinct mechanisms, including DNA mutations^{19,20} and methylation of promoters²¹. A growing number of PTMs have been identified on p16^{9–12}. However, their functions in the control of p16 during cell apoptosis and senescence remain largely unclear. A previous study showed that both expression and phosphorylation level of p16 were elevated in aging prostate cells, and the phosphorylated p16 exhibited an increased binding affinity to CDK4/6⁹. Subsequently, Ser 7, 8, 140 and 152 of p16 have been identified as phosphorylation sites in WI-38 cells. The phosphorylation of Ser 152 appeared to be important for binding of CDK4 to p16, whereas Ser 8 phosphorylation impaired this interaction^{10,11}. In this study, we showed p16S8A and p16S140A mutants relieved the cell cycle arrest and apoptosis induced by p16. In contrast, p16S152A mutant led to an opposite outcome (Fig. 1B and C). These observations imply that the phosphorylation of different residues may have different physiological functions. Furthermore we have previously shown that specific arginine residues of p16 protein are methylated by PRMT6, resulting in impaired p16-CDK4 association as well as alleviated cell cycle arrest at G1¹². Therefore, distinct PTMs on p16 may control p16 function in different manners.

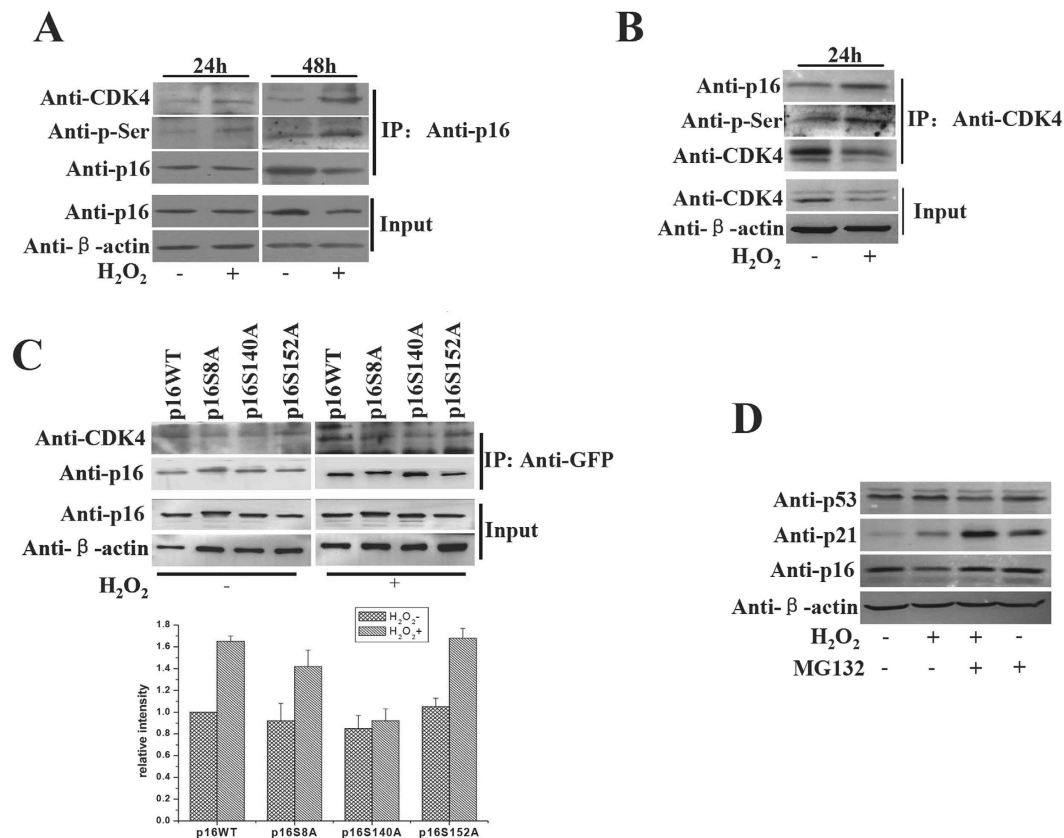


Figure 3. Phosphorylated p16 protein had an enhanced association with CDK4. 293T cells were treated with 1 mM H₂O₂ 24 h or 48 h. Whole-cell extracts were prepared and immunoprecipitated with anti-p16 antibody (A) or anti-CDK4 antibody (B). Precipitates were subjected to immunoblotting with anti-p16, anti-CDK4 and anti-phosphoserine antibodies. (C) 293T cells were transfected with wild type p16-GFP or mutant p16-GFP expression plasmids, and after 24 h treated with 1 mM H₂O₂. After 24 h whole-cell extracts were prepared and immunoprecipitated with anti-GFP antibody. Precipitates were subjected to immunoblotting with anti-p16 and anti-CDK4 antibodies. Upper: The western of p16, CDK4 and actin as indicated. Lower: the results was photodensitometry analysis of the western bands from three experiments, and the results are presented as the relative intensity ratio between CDK4 bands and IP-p16 bands. (D) Western blot analysis of the p16, p21 and p53 proteins in 293T cells treated with 1 mM H₂O₂ or 20 μM MG132 or H₂O₂ together with MG132, then cultured 48 h.

It has been shown that the arginine residues of FOXO1 and BAD were methylated by PRMT1, and the methylation in turn blocked Akt-mediated serine phosphorylation^{13,14}. Another recent study demonstrated that Arg 1173 methylation increased trans-autophosphorylation at Tyr 1173 of EGFR¹⁵. These evidence suggest that crosstalk between arginine methylation and serine phosphorylation may be crucial for the control of protein functions. Here, we found that p16R138K overexpression in 293T cells was associated with an increase of G1 cells, while the overexpression of p16S140A led to a reduction of G1 cells. When cells were transfected with p16S140A/R138K, the population of G1 cells was largely unaffected as compared to that in cells overexpressing wild type p16 (Fig. 1B). Moreover, arginine methylation of p16 was upregulated when S140 was mutated to alanine. We also observed elevated serine phosphorylation of p16 as R138 was replaced by a lysine (Fig. 4B and C). Consistent with previous reports^{13,14}, these results suggest an antagonistic effect existing between Arg 138 methylation and Ser 140 phosphorylation on p16.

Oxidative stress is involved in the death of neurons and leads to the apoptosis in the neurological diseases²². ROS may be the first-stage initiators inducing neuron apoptosis or act as a signal in apoptotic cascade^{23,24}. As a typical ROS, hydrogen peroxide (H₂O₂) is widely used as an apoptosis inducer¹⁶. It has been shown that H₂O₂ induced DNA damage and apoptosis in human neuroblastoma SK-N-MC cells²⁵. H₂O₂ could also elicit Ca²⁺ influx through store-operated channels (SOCs) in HEK-293 cells²⁶. Moreover, p16 level was rapidly upregulated in a p38 stress-activated protein kinase-dependent manner upon H₂O₂-induced oxidative stress²⁷. It has also been demonstrated that the H₂O₂-induced senescence in NHEKs and HepG2 cells is due to the enhanced p16 expression mediated by suppressed methylation on p16 promoter^{28,29}. These data suggest that different mechanisms associated with p16 function may be involved in H₂O₂-induce cell senescence and apoptosis. Here we found that H₂O₂ induced cell apoptosis in a dose-dependent manner (Fig. 2A). Endogenous p16 was substantially phosphorylated upon H₂O₂ treatment (Fig. 2D) and NAC reduced the H₂O₂-induced phosphorylation of p16 (Fig. 2E). Importantly, we provided evidence that the phosphorylation of p16 improved the binding affinity of p16 with

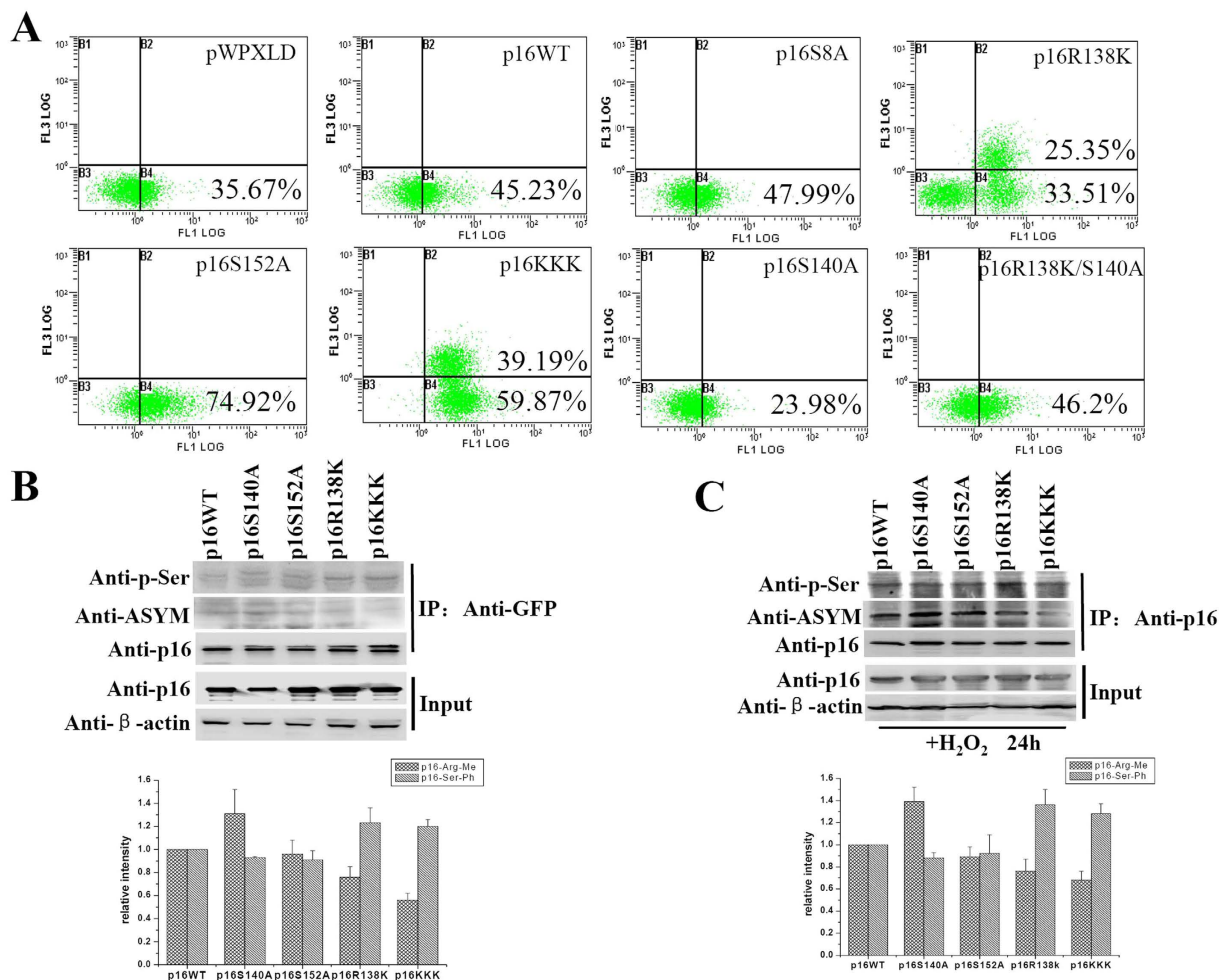


Figure 4. The antagonistic crosstalk between Ser 140 phosphorylation and Arg 138 methylation of p16 protein. (A) 293T cells were transfected with empty control vector (pWPXLD), wild type p16, or mutant p16 expression plasmids. After 24 h the cells were treated with 1 mM H₂O₂ for 30 min, and after 24 h the apoptosis was evaluated by flow cytometry. Apoptosis rates were calculated on the basis of 15 000 cells. (B,C) CoIP assays with anti-GFP or anti-p16 and detected with anti-p16, anti-ASYM or anti-phosphoserine antibody. 293T cells transfected with wild type p16 or mutant p16 expression plasmids. After 24 h the cells were treated with 1 mM H₂O₂ for 30 min, and cultured 24 h before harvest. Upper: The western of p16, methylated-p16, phosphorylated-p16 and actin as indicated. Lower: The results were the photodensitometry analysis of the western bands from three experiments, and the results are presented as the relative intensity ratio between phosphorylation or methylation bands and IP-p16 bands.

CDK4 (Fig. 3A). These results suggest that H₂O₂ enhances the phosphorylation of p16 protein, which in turn influences cell cycle as well as apoptosis. In addition, we found that H₂O₂ effectively promoted p16 phosphorylation and cell senescence in WI-38 (Fig. 5A,B and C). We thus speculate that the phosphorylation of p16 promoted is involved in H₂O₂-induced cell apoptosis and senescence. p16 has previously been shown to have a relatively short half-life ranging from 30 min to 3.5 h in a variety of cancer cell lines³⁰. A direct interaction with REG-γ could also facilitate p16 degradation³¹. p16 can probably be subjected to ubiquitination-mediated proteasomal degradation when it is phosphorylated³². In agree with this observation, we showed that the p16 level was reduced in response to H₂O₂ treatment and restored by the proteasome inhibitor MG132 (Fig. 3D). This suggests that H₂O₂ is able to promote the degradation of p16 proteins.

In summary, we have provided evidence that H₂O₂ induces the phosphorylation of p16 protein, which enhances CDK4 association. Meanwhile, the phosphorylated p16 is degraded probably by ubiquitination-mediated proteasomal system (Fig. 6). Furthermore, our data support an antagonistic crosstalk between the Ser 140 phosphorylation and the Arg 138 methylation on p16. These findings will pave the way to future therapeutic treatment associated with functional targeting of p16.

Methods

Cell culture and transient transfection. The cell lines (293T and WI-38) were cultured in DMEM supplemented with 10% FBS (fetal bovine serum), 100 U/ml penicillin and 100 μg/ml streptomycin, and kept in a

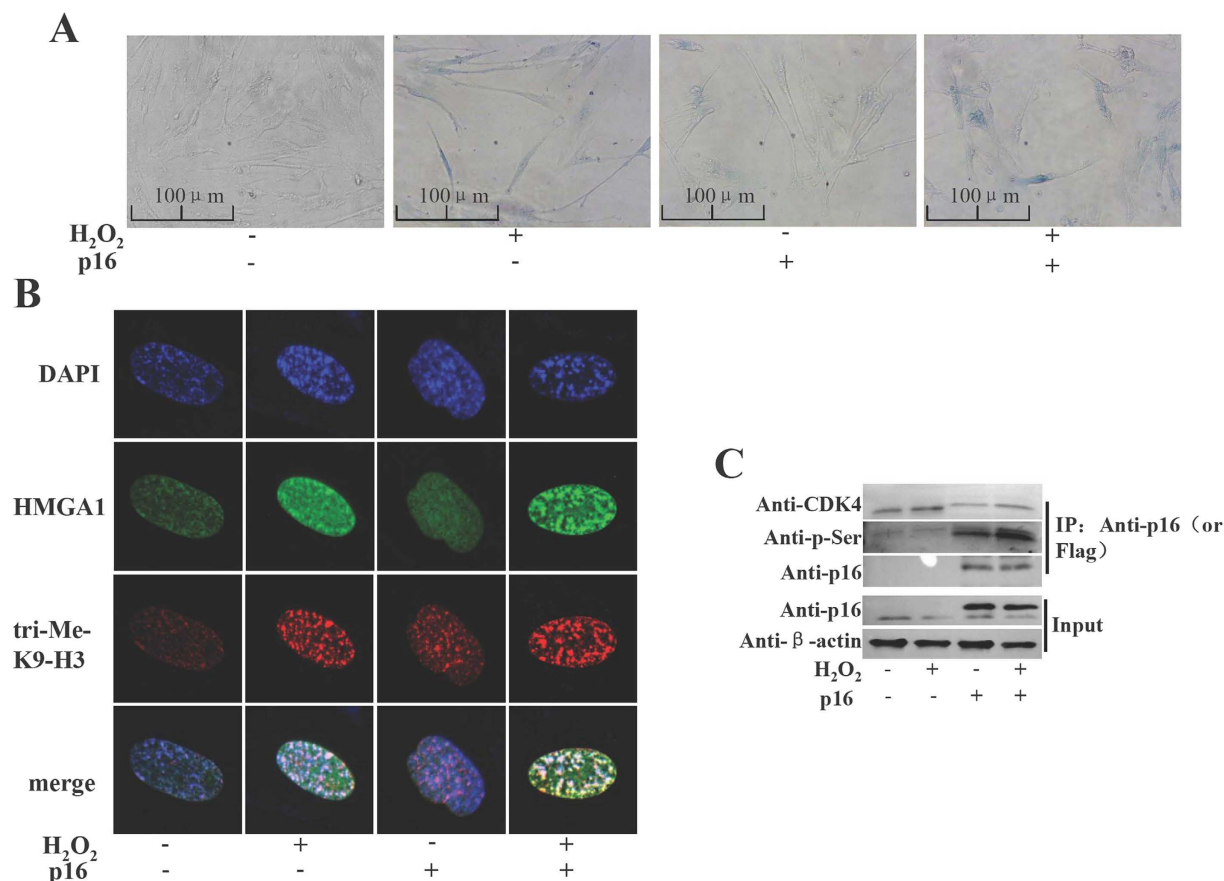


Figure 5. H_2O_2 induced the senescence and p16 phosphorylation in WI-38 cells. (A) WI-38 cells were transfected with empty control vector (pWPXLD), or wild type p16 expression plasmids. After 24 h the cells were treated with 1 mM H_2O_2 for 30 min and then cultured 3 days. The cells were treated with 1 mM H_2O_2 for 30 min again. After 3 days representative photomicrographs of the SA- β -gal staining are detected under a microscope. (B) Cells were stained with DAPI, and the heterochromatic foci were visualized by fluorescence microscopy. The 3meK9H3 was immunostained in red, and HMGA1 in green. The nuclei were counterstained with DAPI (blue). The cells were visualized under a confocal microscope. (C) the WI-38 cells transfected with plasmids indicated and treated with H_2O_2 as described above. CoIP with anti-p16 or anti-Flag, and detected with anti-CDK4, anti-p16 or anti-phosphoserine antibody. Input: proteins prior to immunoprecipitation.

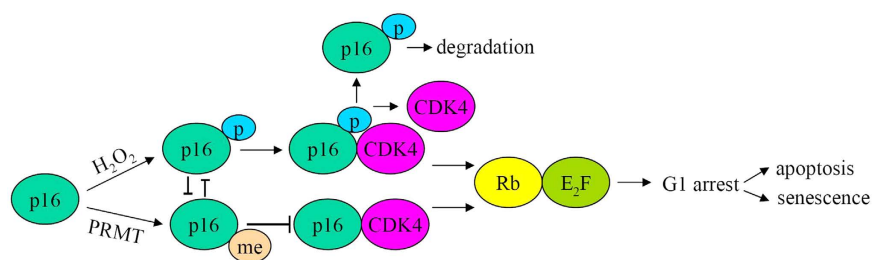


Figure 6. Model for phosphorylation and degradation of p16 induced by H_2O_2 . Firstly, H_2O_2 induced phosphorylation of p16, and then the phosphorylated p16 interacted with CDK4. p16-CDK4 facilitate the stabilization of Rb-E₂F₁, thereby leading to the cell cycle arrest at G1 phase. Subsequently the phosphorylated-p16 was degraded. However, the methylated p16 decrease the formation of p16-CDK4 complexes. Arrows and bars represent positive and negative regulation, respectively. Me denotes methylation; P denotes phosphorylated.

humidified atmosphere containing 5% CO_2 at 37°C. Cells were incubated in culture medium with or without H_2O_2 (0.6 mM, 0.8 mM, 1 mM, 1.2 mM or 1.4 mM) for 30 min, and then cultured 24 h or 48 h in the medium without H_2O_2 . The transfection of WI-38 and 293T cells was carried out using the Lipofectamine 2000 reagent (Invitrogen) or the PEI reagent (Sigma).

Plasmids. The p16-EGFP-N1 plasmid was provided by Dr. Jun Chen (New York Medical College, USA). The specific site mutations of the arginine or serine residues were introduced into the p16 cDNA region by using a two-step PCR procedure. Two simultaneous PCR reactions, using p16-EGFP-N1 as template, were performed. Amplified fragments from each PCR reaction were purified, mixed, and subjected to a second round of PCR using two external primers. The mutagenic sequence for the Ser 8 residue was AGC (Serine) to GCC (Alanine), for the Ser 140 residue was AGT (Serine) to GCT (Alanine), and for the Ser 152 residue was TCA (Serine) to GCA (Alanine). The amplified PCR products were inserted into the *HindIII* and *BamHI* sites of EGFP-N1 vector, and the correct insertion was verified by DNA sequencing. The arginine residue mutations of p16 vectors were described previously¹². Then, these p16 cDNAs including specific site mutations of the arginine or serine residues, were amplified using PCR reaction and the Flag tag were introduced into the PCR products, which were inserted into the *PmeI* and *SpeI* sites of pWPXLD vector.

Western blotting and co-immunoprecipitation (CoIP). Endogenous expression of p16, p21 and p53 proteins was detected by Western blotting. 293T cells were treated with 30 mM NAC (antioxidant N-acetyl-L-cysteine) for 2 h and then 1 mM H₂O₂ was added. After 30 min the cells were cultured in normal medium for 48 h. 1×10^6 cells were digested and lysed in lysis buffer (50 mM Tris-HCl, pH 8.0; 150 mM NaCl; 0.5% NP-40; 1 mM EDTA; protease inhibitors cocktail) for 30 min at 4 °C after they were washed twice with PBS buffer. Total cell extracts were separated in 15% SDS-polyacrylamide gel electrophoresis (PAGE), then transferred to a polyvinylidene fluoride membrane. The membrane was incubated with anti-p53 (Sigma, p6495), anti-p16 (BD, 551154), anti-21 (Santa cruz, sc-756), or anti- β -actin (Sigma, A1978) antibodies, and visualized by using the Chemiluminescent Substrate method with the SuperSignal West Pico kit provided by Pierce Co. β -actin was used as an internal control for normalizing the loading materials.

Co-precipitation of p16 with CDK4 was performed in 293T cells. Cells were lysed in lysis buffer (50 mM Tris-HCl, pH 8.0; 150 mM NaCl; 0.5% NP-40; 1 mM EDTA; protease inhibitor cocktail). Total cell extracts were incubated with the anti-GFP (Abcam, ab1218), anti-CDK4 (Santa Cruz, sc-260) and anti-p16 antibodies, with gentle shaking for 1 h at 4 °C, followed by the addition of 40 μ l of Protein A-agarose and an incubation for another 3 h. The pellets were collected and washed twice with Buffer A (20 mM Tris-HCl, pH 8.0; 10 mM NaCl; 0.5% NP-40; 1 mM EDTA). The beads were resuspended in 50 μ l of 5 \times loading buffer and boiled for 10 min. The proteins were separated in a 12% or 15% SDS-PAGE gel and then transferred to polyvinylidene fluoride membrane for immunoblotting detection with anti-p16, anti-CDK4, anti-phosphoserine (Millipore, ab1603) or anti-dimethyl-arginine (asymmetric) (Millipore, 07-414, ASYM24) antibodies.

Flow cytometric analysis. 293T cells were trypsinized and washed with cold PBS once and then fixed in 70% ethanol and stored at 4 °C for 30 min. Fixed cells were washed with PBS and suspended in 100 μ l of PBS, added with 1 μ l 10 mg/ml RNAaseA and 100 μ l propidium iodide. Stained cells were incubated at room temperature for 30 min in the dark. The cellular DNA content was quantified by flow cytometric analysis using a FACS Calibur (Beckman coulter, USA). The apoptosis assay was performed by using the annexin V-fluorescein isothiocyanate (FITC) apoptosis detection kit (Nanjingkaiji, Nanjing, China), and detected by flow cytometry (excitation at 488 nm; emission at 530 nm) with an FITC signal detector, and propidium iodide (PI) staining with a phycoerythrin emission signal detector.

Senescence-associated galactosidase activity assay. WI-38 cells were transfected with the p16 expression vectors. After 24 h, the cells were treated with 1 mM H₂O₂ for 30 min, and then cultured in normal medium. At day 3 after treatment, cells were treated with H₂O₂ for another 3 days. Cells were then processed using a Senescence β -Galactosidase Staining Kit (Cell Signaling Technology), before they were examined under a light microscope (Nikon, Japan) and the images were collected at $\times 20$ magnification with appropriate filters. These experiments were repeated three times, and one of the representative results is shown.

Immunofluorescence staining. WI-38 cells were transfected with the p16 expression vectors. After 24 h, the cells were treated with 1 mM H₂O₂ for 30 min, and then cultured in the normal medium. At day 3 after treatment, cells were treated with H₂O₂ for another 3 days. The treated WI-38 cells were washed twice in PBS, fixed with 4% paraformaldehyde for 15 min, permeabilized with 0.2% Triton X-100 at room temperature and then quenched in ice-cold PBS. Trimethylated histone H3 was detected with anti-3meK9H3 antibody (Mollipore, 07-523) and visualized with a TRITC-conjugated anti-rabbit IgG secondary antibody (Zhongshan, China), and then incubated with anti-HMGAI (Sigma, SAB1401183) antibody serum for 1 h and visualized with a FITC-conjugated secondary antibody. Finally, cells were stained with DAPI before they were visualized under an Olympus FV1000 (Olympus, Japan) confocal microscope.

Mitochondrial ROS assay. 293T cells were trypsinized and washed with PBS once and then incubate with 1 ml 5 μ M MitoSOXTM reagent (M36008, invitrogen) for 10 min at 37 °C in the dark. Then wash cells gently three times with PBS, and detected by flow cytometry (excitation at 488 nm; emission at 580 nm).

Mitochondria membrane potential ($\Delta\Psi$ m) assay. Mitochondria membrane potential was determined with JC-1 (Beyotime Biotech, Nantong, China). Briefly, 293T cells were seeded in 60 mm plates. After experimental treatment, cells were trypsinized and washed with PBS once, and then added with 1 ml staining dye and incubated at 37 °C for 20 min. After this, cells were washed twice with cold JC-1 staining buffer (1 \times), and detected by flow cytometry (excitation at 488 nm; emission at 529 nm).

References

1. Ruas, M. & Peters, G. The p16INK4a/CDKN2A tumor suppressor and its relatives. *Biochim. Biophys. Acta.* **1378**, 115–177 (1998).
2. Sharpless, N. E. INK4a/ARF: A multifunctional tumor suppressor locus. *Mutat. Res.* **576**, 22–38 (2005).
3. Ortega, S., Malumbres, M. & Barbacid, M. CyclinD-dependent kinases, INK4 inhibitors and cancer. *Biochim. Biophys. Acta.* **1602**, 73–89 (2002).
4. Li, J. *et al.* Structure-function relationship of the INK4 family of tumor suppressors. In *DNA Alterations in Cancer: Genetic and Epigenetic Changes* (Ehrlich, M., Ed.) 71–83 (2000).
5. Sang, Y. *et al.* LncRNA PANDAR regulates the G1/S transition of breast cancer cells by suppressing p16INK4A expression. *Sci. Rep.* **6**, 22366 (2016).
6. Wang, X. *et al.* P300 plays a role in p16 (INK4a) expression and cell cycle arrest. *Oncogene* **27**, 1894–1904 (2008).
7. Wang, X. *et al.* YY1 restrained cell senescence through repressing the transcription of p16. *Biochim. Biophys. Acta.* **1783**, 1876–1883 (2008).
8. Feng, Y. *et al.* The transcription factor ZBP-89 suppresses p16 expression through a histone modification mechanism to affect cell senescence. *FEBS J.* **276**, 4197–4206 (2009).
9. Sandhu, C., Peehl, D. M. & Slingerland, J. p16INK4A mediates cyclin dependent kinase 4 and 6 inhibition in senescent prostatic epithelial cells. *Cancer Res.* **60**, 2616–2622 (2000).
10. Gump, J., Stokoe, D. & McCormick, F. Phosphorylation of p16INK4A correlates with Cdk4 association. *J. Biol. Chem.* **278**, 6619–6622 (2003).
11. Guo, Y., Yuan, C., Weghorst, C. M. & Li, J. IKKbeta specifically binds to P16 and phosphorylates Ser8 of P16. *Biochem. Biophys. Res. Commun.* **393**, 504–508 (2010).
12. Wang, X. *et al.* Suppression of PRMT6-mediated arginine methylation of p16 protein potentiates its ability to arrest A549 cell proliferation. *Int. J. Biochem. Cell Biol.* **44**, 2333–2341 (2012).
13. Yamagata, K. *et al.* Arginine methylation of FOXO transcription factors inhibits their phosphorylation by Akt. *Mol. Cell* **32**, 221–231 (2008).
14. Sakamaki, J. *et al.* Arginine methylation of BCL-2 antagonist of cell death (BAD) counteracts its phosphorylation and inactivation by Akt. *PNAS* **108**, 6085–6090 (2011).
15. Hsu, J. M. *et al.* Crosstalk between Arg 1175 methylation and Tyr 1173 phosphorylation negatively modulates EGFR-mediated ERK activation. *Nat. Cell Biol.* **13**, 174–181 (2011).
16. Sato, T., Kaneko, Y. K., Sawatani, T., Noguchi, A. & Ishikawa, T. Obligatory Role of Early Ca(2+) Responses in H2O2-Induced beta-Cell Apoptosis. *Biol. Pharm. Bull.* **38**, 1599–1605 (2015).
17. Rayess, H., Wang, M. B. & Srivatsan, E. S. Cellular senescence and tumor suppressor gene p16. *Int. J. Cancer* **130**, 1715–1725 (2011).
18. Otterson, G. A., Kratzke, R. A., Coxon, A., Kim, Y. W. & Kaye, F. J. Absence of p16INK4 protein is restricted to the subset of lung cancer lines that retains wildtype RB. *Oncogene* **9**, 3375–3378 (1994).
19. Mori, T. *et al.* Frequent somatic mutation of the MTS1/CDK4I (multiple tumor suppressor/cyclin-dependent kinase 4 inhibitor) gene in esophageal squamous cell carcinoma. *Cancer Res.* **54**, 3396–3397 (1994).
20. Nobori, T. *et al.* Deletions of the cyclin-dependent kinase-4 inhibitor gene in multiple human cancers. *Nature* **368**, 753–756 (1994).
21. Mao, L. *et al.* A novel p16INK4A transcript. *Cancer Res.* **55**, 2995–2997 (1995).
22. Naoi, M. *et al.* Mitochondria in neurodegenerative disorders: regulation of the redox state and death signaling leading to neuronal death and survival. *J. Neural Transm (Vienna)* **116**, 1371–1381 (2009).
23. Kruman, I., Bruce-Keller, A. J., Bredesen, D., Waeg, G. & Mattson, M. P. Evidence that 4-hydroxynonenal mediates oxidative stress-induced neuronal apoptosis. *J. Neurosci.* **17**, 5089–5100 (1997).
24. Valencia, A. & Moran, J. Role of oxidative stress in the apoptotic cell death of cultured cerebellar granule neurons. *J. Neurosci. Res.* **64**, 284–297 (2001).
25. Choi, D. J., Kim, S. L., Choi, J. W. & Park, Y. I. Neuroprotective effects of corn silk maysin via inhibition of H2O2-induced apoptotic cell death in SK-N-MC cells. *Life Sci.* **109**, 57–64 (2014).
26. Bogeski, I., Bozem, M., Sternfeld, L., Hofer, H. W. & Schulz, I. Inhibition of protein tyrosine phosphatase 1B by reactive oxygen species leads to maintenance of Ca2+ influx following store depletion in HEK 293 cells. *Cell Calcium.* **40**, 1–10 (2006).
27. Noah, C. J., Tong, L., Pamela, C. & Sancy, A. L. The p16INK4A tumor suppressor regulates cellular oxidative stress. *Oncogene* **30**, 265–274 (2011).
28. Sasaki, M., Kajiyama, H., Ozeki, S., Okabe, K. & Ikebe, T. Reactive oxygen species promotes cellular senescence in normal human epidermal keratinocytes through epigenetic regulation of p16 (INK4a). *Biochem. Biophys. Res. Commun.* **452**, 622–628 (2014).
29. Lim, J. S., Park, S. H. & Jang, K. L. Hepatitis C virus Core protein overcomes stress-induced premature senescence by down-regulating p16 expression via DNA methylation. *Cancer Lett.* **321**, 154–161 (2012).
30. Gombart, A. F., Yang, R., Campbell, M. J., Berman, J. D. & Koeffler, H. P. Inhibition of growth of human leukemia cell lines by retrovirally expressed wild-type p16INK4A. *Leukemia* **11**, 1673–1680 (1997).
31. Chen, X., Barton, L. F., Chi, Y., Clurman, B. E. & Roberts, J. M. Ubiquitin-independent degradation of cell-cycle inhibitors by the REGgamma proteasome. *Mol. Cell* **26**, 843–852 (2007).
32. Li, J., Poi, M. J. & Tsai, M. D. Regulatory mechanisms of tumor suppressor P16(INK4A) and their relevance to cancer. *Biochemistry* **50**, 5566–5582 (2011).

Acknowledgements

This work was supported by the National Natural Science Foundation of China (31271442 and 31571317).

Author Contributions

X. Wang and J. Lu conceived the study. Y. Lu and W. Ma performed all experiments. Z. Li helped to prepare the samples. X. Wang wrote the manuscript.

Additional Information

Supplementary information accompanies this paper at <http://www.nature.com/srep>

Competing financial interests: The authors declare no competing financial interests.

How to cite this article: Lu, Y. *et al.* The interplay between p16 serine phosphorylation and arginine methylation determines its function in modulating cellular apoptosis and senescence. *Sci. Rep.* **7**, 41390; doi: 10.1038/srep41390 (2017).

Publisher's note: Springer Nature remains neutral with regard to jurisdictional claims in published maps and institutional affiliations.



This work is licensed under a Creative Commons Attribution 4.0 International License. The images or other third party material in this article are included in the article's Creative Commons license, unless indicated otherwise in the credit line; if the material is not included under the Creative Commons license, users will need to obtain permission from the license holder to reproduce the material. To view a copy of this license, visit <http://creativecommons.org/licenses/by/4.0/>

© The Author(s) 2017